*Articles*

# EPR Study of the Mixed-Valent Diiron Sites in Mouse and Herpes Simplex Virus Ribonucleotide Reductases. Effect of the Tyrosyl Radical on Structure and Reactivity of the Diferric Center†

Roman M. Davydov,‡,§ Albert Davydov,‡ Rolf Ingemarson,|| Lars Thelander,|| Anders Ehrenberg,‡ and Astrid Gräslund*,‡

*Department of Biophysics, Stockholm University, Arrhenius Laboratory, S-106 91 Stockholm, Sweden, and Department of Medical Biochemistry and Biophysics, Umeå University, S-901 87 Umeå, Sweden*

*Received January 7, 1997; Revised Manuscript Received May 12, 1997*⊗

ABSTRACT: Reduction of ribonucleotide reductase (EC 1.17.4.1) R2 proteins in a frozen glycerol−buffer solution at 77 K by mobile electrons generated by $\gamma$-irradiation produces EPR-detectable iron sites in mixed-valent Fe(II)/Fe(III) states. The primary EPR signals give information about the ligand arrangement of the diferric form of the iron site, whereas secondary signals observed after annealing of the sample show the effects of structural relaxation. In recombinant metR2 proteins (without free radical) from mouse and herpes virus type 1, the mixed-valent sites trapped at 77 K give rise to axial $S = {}^1/_2$ EPR spectra with $g$ values in the range 1.79−1.94, observable at temperatures up to 110 K. The spectra are assigned to $\mu$-oxo-bridged dinuclear iron sites. In mouse metR2, the primary EPR spectrum is a mixture of two components. Annealing the R2 samples to 160−170 K transforms the primary EPR signals into rhombic spectra, characterized by $g_{av} < 1.8$, and observable only below 25 K. These spectra are assigned to partially relaxed forms with a $\mu$-hydroxo bridge, formed by protonation of the oxo bridge. Further annealing at 220 K produces new rhombic EPR spectra, which are closely similar with those observed and found to be stable after chemical reduction at room temperature. The EPR signal of the primary mixed-valent iron site in active mouse R2 protein with a tyrosyl radical also has two components. Both are different from those observed in metR2. In herpes simplex virus type 1 protein R2, one primary mixed-valent component was observed for the met protein. The dose−yield curve for the mixed-valent state in active mouse R2 is sigmoidal in shape, indicating that the tyrosyl radical is reduced by mobile electrons before the iron site. Kinetic experiments on the reduction by dithionite on mouse R2 without and with radical show a significantly enhanced rate for reduction of the iron site in the protein without radical. The results suggest that in active mouse R2 only complete diferric sites with neighboring radicals give rise to the mixed-valent spectra, and that these sites may exist in two structurally distinct forms. The results on the mouse R2 proteins confirm and extend previous results obtained on the *Escherichia coli* protein R2 showing that the presence of the tyrosyl radical significantly affects not only the structure but also the reactivity of the iron site.

Ribonucleotide reductase (RNR, EC 1.17.4.1)[1] catalyzes the reduction of ribonucleotides to the corresponding deoxyribonucleotides (Reichard, 1988; Stubbe, 1990), a reaction necessary for DNA replication. The enzymes from *Escherichia coli*, mammalian cells, and HSV1 [class I RNR, (Reichard, 1993)] are composed of two nonidentical components referred to as proteins R1 and R2 (Fontecave et al., 1992; Eriksson et al., 1989; Mann et al., 1991; Thelander et al., 1994). Each component consists of two identical polypeptide chains. The large component, R1, binds substrates and allosteric effectors and contains sulfhydryl groups responsible for the reduction of the substrate during the enzymatic reaction. The small component, protein R2, contains in each of its two polypeptide chains a site for a tyrosyl radical, essential for the enzymatic activity, and a neighboring $\mu$-oxo-bridged diferric cluster, involved in the generation and stabilization of the radical.

The current information on the structure and chemical reactivity of the redox centers of protein R2 is to a large extent based on studies on *E. coli* RNR. The three-dimensional structure of the *E. coli* R2 protein in its nonradical form (metR2) has been determined by Nordlund et al. (1990, 1993). Recently also the three-dimensional structure of recombinant mouse protein R2 has been reported (Kauppi et al., 1996). In both crystallographic structures of R2, the details of the iron/radical site and its environment

† This work was supported by grants from the Bank of Sweden Tercentenary Foundation, the Swedish Natural Science Research Council, the Magn. Bergvall Foundation, and the Royal Swedish Academy of Sciences.

‡ Stockholm University.

§ Present address: Department of Biochemistry, Chemical Center, Lund University, S-221 00 Lund, Sweden.

|| Umeå University.

⊗ Abstract published in *Advance ACS Abstracts,* July 1, 1997.

[1] Abbreviations: RNR, ribonucleotide reductase; HSV1, herpes simplex virus type 1; metR2, radical-free R2 protein.

S0006-2960(97)00037-8 CCC: $14.00 

are quite similar. The iron center of metR2 contains two inequivalent six-coordinated Fe(III) ions bridged by one $\mu$-oxo and one $\mu$-carboxylate group with additional histidine and carboxylate ligands.

The present study concerns the mixed-valent states of the recombinant mammalian (mouse) and HSV1 R2 proteins. A striking difference between the structures of the *E. coli* and mouse R2 proteins is that in the latter case there is an open channel from the protein surface to the iron site, which should allow direct access of small molecules in the solvent to this site. This would explain the observed differences concerning the enhanced reactivity and sensitivity of the iron/radical centers in the mouse (and HSV1) R2 proteins compared to that in the *E. coli* R2 protein toward reductants, radical scavengers, and iron chelators (Galli et al., 1995; Atta et al., 1993, 1994; Nyholm et al., 1993; Barlow et al., 1983; Lassmann et al., 1992; McClarty et al., 1980; Davydov, A., et al., 1996). The tyrosyl radical and diiron sites in mouse protein R2 are reduced by dithionite (Davydov, A., et al., 1996), while in *E. coli* protein R2 these centers are inaccessible toward this strong reductant. The radical scavenger hydroxyurea reduces the tyrosyl radical in *E. coli* R2 but leaves the iron center intact (Barlow et al., 1983), while in mouse R2 both the free radical and the iron center may be reduced by this agent (Nyholm et al., 1993; McClarty et al., 1980).

The diiron sites in mouse and HSV1 R2 proteins are explored in the present EPR study of their mixed-valent states obtained by reduction in frozen solution at 77 K with mobile electrons generated by $\gamma$-radiolysis. Comparison is made with the *E. coli* R2 protein for which we recently showed (Davydov et al., 1994; Davydov, R., et al., 1996) that high yields of kinetically stabilized mixed-valent diiron sites could be produced and studied under such conditions. The primary mixed-valent Fe(II)/Fe(III) centers produced at 77 K retain a conformation close to that of the original diferric centers (Davydov et al., 1994) and are not allowed to relax because of the significant steric hindrance in the solid matrix at 77 K. The configuration of the metal ion site after one-electron reduction at 77 K is therefore commonly constrained and in a nonequilibrium state. The strong constraints in the primary mixed-valent states in the solid matrix may be successively released by annealing at higher temperatures (Davydov et al., 1994; Davydov, R., et al., 1996). The kinetically stabilized intermediates and the final fate of the mixed-valent diiron center reflect properties of the iron center and its protein environment.

In active *E. coli* R2, the presence of the tyrosyl radical led to a different primary mixed-valent form of the iron site compared to that of the met protein (Davydov R., et al., 1996). In the present study, we have confirmed and expanded the observations on how the tyrosyl radical affects the properties of the neighboring iron site in the mouse R2 protein.

## MATERIALS AND METHODS

The chemicals used were obtained as follows and used without further purification: glycerol (Merck), flavin mononucleotide (FMN) (Sigma), *N*-ethyldibenzopyrazine ethyl sulfate salt (PES) (Sigma), tris(hydroxymethyl)aminomethane (Tris) (Sigma). Deazaflavin was a generous gift of Dr. J. Coves (University Joseph Fourier, Grenoble, France).

Recombinant mouse and HSV1 R2 proteins were prepared, reacted with iron/ascorbate, and desalted as previously reported (Mann et al., 1991). A truncated form of the HSV1 protein R2 lacking the seven carboxyl-terminal amino acid residues GAVVDL was produced according to Filatov et al. (1992). Protein metR2 from *E. coli* was prepared as described in McClarty et al. (1980). The met form of mouse R2 protein was produced by incubation of the radical containing active protein in a buffer−glycerol solution (1:1) with 20 mM hydroxyurea for 30 s followed by rapid freezing at 77 K or by treatment with an equimolar amount of 4-butoxyphenol [$CH_3(CH_2)_3OC_6H_4OH$ from Aldrich] for 60 min at 4 °C (Davydov, A., et al., 1996). Protein metR2 from HSV1 was prepared by incubation of the active protein in a buffer−glycerol solution (1:1) with 20 mM hydroxyurea for 30 s followed by rapid freezing at 77 K. The concentrations of the mouse and HSV1 R2 proteins were determined spectrophotometrically using the known extinction coefficients at 280 nm (124 000 $M^{-1}$ $cm^{-1}$ for mouse R2 and 104 000 $M^{-1}$ $cm^{-1}$ for HSV1 R2) (Mann et al., 1991). Typically, the mouse protein R2 had an iron and tyrosyl radical content of about 4 Fe/R2 and 1 radical/R2, respectively. The HSV1 R2 protein had comparable iron content, but less radical, only about 0.15 radical/R2 [cf. Mann et al. (1991)].

Protein solutions were prepared in 50 mM Tris-HCl, 100 mM KCl buffer (pH 7.6) and mixed with half or equal volumes of glycerol. The final protein concentrations of the samples were in the range 0.6−1.1 mM. $\gamma$-Irradiation of samples was performed in quartz tubes, 3.5−4 mm diameter, immersed in liquid $N_2$ in a dewar which was placed in a $^{137}Cs$ source giving a dose rate of 65 krad/h.

EPR studies were made on samples exposed to 2.5−4.5 Mrad radiation doses unless otherwise stated. Annealing of the samples irradiated at 77 K was performed in a cooled *n*-pentane bath at suitable temperatures followed by recooling at 77 K.

Mixed-valent forms of the mouse and HSV1 proteins stable at room temperature were produced photochemically using the following photoreaction mixtures: (a) 20 mM glycine (reductant) + 0.2 mM FMN (photosensitizer) + 0.3 mM PES (mediator); or (b) 50 mM Tris (reductant) + 0.03 mM deazaflavin (photosensitizer) + 0.1 mM PES. A 0.2 mL aliquot of anaerobic 0.2−0.5 mM protein solution in buffer−glycerol (4:1) containing the photoreaction mixture in a quartz tube was exposed to white light from a projector with a 150 W halogen lamp for 3−5 min. To prevent protein denaturation, all operations with photoreduction were performed at 4 °C. Anaerobic samples were made by repeated cycles of evacuation and flushing with $O_2$-free argon gas.

EPR spectra were recorded using a Bruker ESP300 X-band spectrometer equipped with a cold finger dewar at 77 K, a nitrogen flow system for temperatures between 77 and 130 K, or an Oxford Instruments ESR9 liquid helium cryostat for temperatures between 3.6 and 50 K. Spin quantitations were made by comparison with a standard sample, a solution of 1 mM $Cu(ClO_4)_2$, and performing double integrations of spectra measured at nonsaturating microwave power levels by means of standard Bruker software.

Power saturation data were obtained from the EPR absorption derivative signal intensity, $I$, as a function of incident microwave power, $P$. The data were analyzed using the equation $\log (I/P^{1/2}) = a - (b/2)(\log P_{1/2} - \log P)$ from

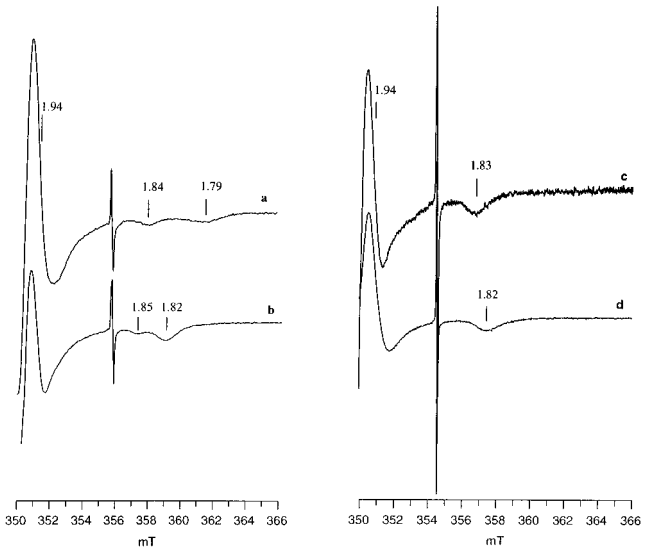


FIGURE 1: EPR spectra of mixed-valent diiron centers produced radiolytically by $\gamma$-irradiation at 77 K in 0.43 mM mouse metR2 (a), 0.43 mM active mouse R2 (b), 0.6 mM HSV1 metR2 (c), and 1 mM *E. coli* metR2 (d). Solvent: 1/1 mixture of glycerol and 50 mM Tris-HCl, pH 7.6, 0.1 M KCl. Irradiation dose: 3.5 Mrad (a), 5 Mrad (b), 2.5 Mrad (c), and 3.65 Mrad (d). Instrument settings: modulation frequency, 100 kHz; modulation amplitude, 5 G; microwave power and temperature, 30 mW, 45 K (a); 10 mW, 20 K (b); 10 mW, 77 K (c and d).

which the half-saturation power, $P_{1/2}$, was determined graphically (Sahlin et al., 1986; Hales, 1993).

Kinetic studies on the reduction of the tyrosyl radical and iron centers in mouse R2 protein with dithionite were followed spectrophotometrically under anaerobic conditions using a Varian Cary 4 spectrophotometer. All studies were carried out in anaerobic semimicrocuvettes. A cuvette was filled with 0.6 mL of 10−12 $\mu$M solution of the protein in 50 mM Tris/HCl and 0.10 M KCl (pH 7.5) containing 10 vol % glycerol. The cuvette capped with a rubber septum was deaerated by flushing argon for 15 min at 0 °C. The reaction was started by addition of 5−10 $\mu$L of anaerobic concentrated solution of dithionite with a gas-tight Hamilton syringe. The reaction involving reduction of the tyrosyl radical was monitored at 414 nm, while combined tyrosyl radical and diiron(III) site reduction was monitored at 380 nm. For simplifying the kinetic analysis in all experiments, the ratio [reductant]/[protein] was kept higher than 5.

## RESULTS

*Mixed-Valent Diiron Sites in Radical-Free Mouse and HSV1 R2 Proteins.* The met form of mouse R2 protein was obtained either by treatment with hydroxyurea or by treatment with 4-butoxyphenol (Davydov, A., et al., 1996), as described under Materials and Methods. Light absorption spectra indicated the presence of an intact iron center (Davydov, A., et al., 1996; cf. also Figure 5B, trace a). Both treatments gave met protein which responded similarly to low-temperature reduction. Figure 1 shows the EPR spectra of the met forms of mouse and HSV1 R2 proteins after reduction by exposure to $\gamma$-radiation at 77 K. For comparison, the EPR spectrum of similarly treated *E. coli* metR2 protein is also presented in the figure (Davydov et al., 1994). Besides the very strong free radical signals centered at $g = 2.0$ (not shown), axial signals with $g_{av} < 2.0$ are clearly visible. The EPR signal of the irradiated mouse metR2 is

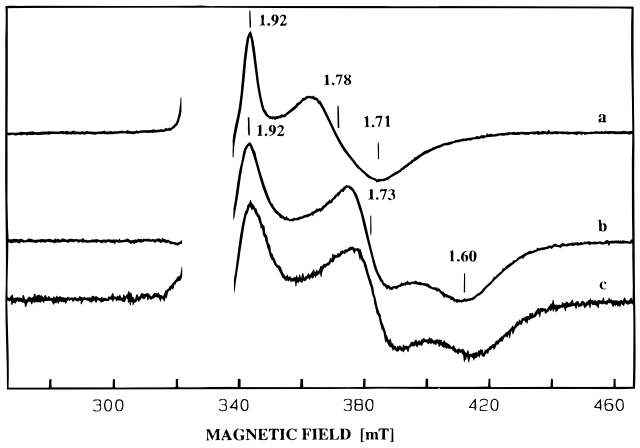


FIGURE 2: EPR spectra of the mixed-valent diiron sites of mouse metR2 obtained by annealing the sample of Figure 1a at 165 K (a) and 220 K (b) or by photochemical reduction at 273 K (c). The experimental conditions and instrument settings as in Figure 1 with microwave power 10 mW and temperature 4 K.

characterized by $g_\perp = 1.94$ and a $g_{||}$ feature which is composed of two negative peaks of about equal amplitude with $g_{||}$ values 1.84 and 1.79 (Figure 1a). In the case of the HSV1 metR2 protein, only one component is seen with $g_\perp = 1.94$ and $g_{||} = 1.83$ (Figure 1c).

These EPR spectra of the primary mixed-valent forms of mouse and HSV1 metR2 proteins are similar to that for the *E. coli* metR2 protein in a mixed-valent state produced by cryogenic reduction (Figure 1d) (Davydov et al., 1994), and may be observed without noticeable broadening at temperatures as high as 110 K. They are saturated at relatively low levels of microwave power at temperatures $\leq$25 K. At 11 K, the half-saturation power, $P_{1/2}$, was found to be 0.5 $\pm$ 0.1 mW and 0.4 $\pm$ 0.1 mW for mouse and HSV1 proteins, respectively, in close agreement with $P_{1/2} = 0.5 \pm 0.1$ mW obtained under similar conditions for the *E. coli* protein R2 (Davydov et al., 1994). In *E. coli* metR2 and methemerythrin (Davydov et al., 1994) and in $\mu$-oxo-bridged model compounds (Davydov, R., et al., 1997), EPR spectra of this type were also obtained after cryogenic reduction. In analogy with these studies the spectra now observed with the mouse and HSV1 R2 proteins are assigned to $S = {}^1/_2$ mixed-valent diiron centers with $\mu$-oxo-bridged antiferromagnetically-coupled high-spin ferric ($S = {}^5/_2$) and high-spin ferrous ($S = 2$) ions, which have a ligand configuration close to that in the original diferric state (Davydov et al., 1994). In the case of mouse metR2, some uncertainty has remained whether treatment of active R2 with hydroxyurea or 4-butoxyphenol really produced intact $\mu$-oxo-bridged diferric centers, since the product had low stability and this type of center is not uniquely characterized by its light absorption spectrum (Davydov, A., et al., 1996). The present results of low-temperature reduction removed, however, any doubts about the presence of $\mu$-oxo-bridged antiferromagnetically-coupled diferric sites in the samples treated with hydroxyurea or 4-butoxyphenol.

Annealing the low-temperature reduced mouse metR2 at 160−170 K for 5−10 min results in a transformation of the primary axial EPR signals (Figure 1a) into a new apparently single-component spectrum with a strong rhombic character and apparent $g$-values 1.92, 1.78, and 1.71 (Figure 2a). This spectrum is significantly broadened already at 20 K and becomes undetectable at temperatures higher than 30 K. The

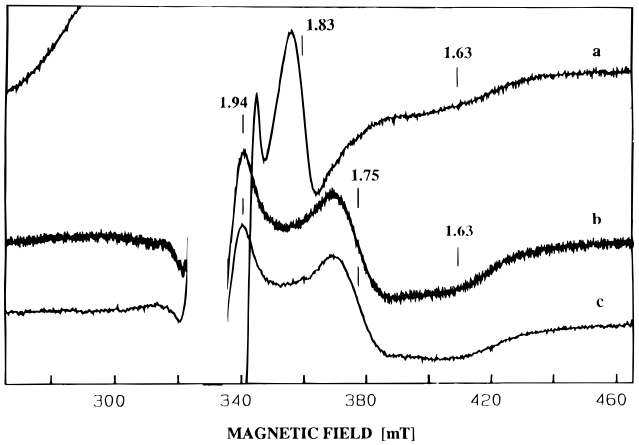


FIGURE 3: EPR spectra of the mixed-valent diiron sites in HSV1 metR2 produced by annealing the sample of Figure 1c at 170 K (a) and 250 K (b) or by photochemical reduction at 273 K (c). The experimental conditions and instrument settings as in Figure 2.

half-saturation power, $P_{1/2}$, for this signal was found to be 1 ± 0.2 mW at 3.6 K and 36 ± 10 mW at 6.3 K. A new spectroscopically distinct mixed-valent species appears after further annealing of the sample at 220 K for 3 min. This species shows an $S = {}^1/_2$ rhombic EPR signal with $g$-values 1.92, 1.73, and 1.60 (Figure 2b), which is observable only at temperatures lower than 25 K. $P_{1/2}$ for this species was found to be 15 ± 5 mW at 3.6 K. This final mixed-valent species obtained from mouse metR2 proved to be stable at room temperature. Quantitation versus a copper standard sample indicates that about 20% of the diiron centers account for the EPR signal of Figure 2b.

Figure 2c shows the EPR spectrum of mouse protein R2 in a mixed-valent state generated by photoreduction using FMN and phenazine ethosulfate as photosensitizer and mediator, respectively. The EPR spectrum of this mixed-valent species is closely similar to that of the mixed-valent species which appears after annealing at 220 K of the mouse metR2 reduced at 77 K (Figure 2b). These two methods of preparation thus result in formation of one and the same species of mixed-valent mouse R2, which was previously also obtained by chemical reduction using dithionite and PMS as mediator (Atta et al., 1994). In contrast, we failed to generate any EPR-detectable mixed-valent species of *E. coli* R2 protein photochemically at 5−30 °C using deazaflavin as photosensitizer with various mediators (phenazine ethosulfate, benzylviologen, and phenosaphranine). Analogously, the mixed-valent species induced by low-temperature reduction in *E. coli* R2 is thermodynamically unstable, and no visible EPR signal was observed after annealing at 230 K (Davydov et al., 1994).

A similar sequence of conversions as with the mouse R2 protein was observed upon annealing the low-temperature reduced HSV1 met protein R2 (Figure 3a,b). Annealing the low-temperature irradiated metR2 at 167 K for 10 min gives rise to a new rhombic signal (Figure 3a) with apparent $g$-values ≥1.91 (quite uncertain because of severe overlap from the strong free radical signal at $g = 2$), 1.83, and 1.63, observable only at temperatures lower than 25 K. A new mixed-valent species appeared upon annealing at 250 K (Figure 3b). This species was found to be stable at 0 °C for more than 10 min. The EPR signal of this latter species is characterized by $g = 1.94$, 1.75, and 1.63 and was only observable at temperatures lower than 20 K. The quantitation

Table 1: Selected Parameters for EPR Spectra of the Primary Mixed-Valent Forms of Ribonucleotide Reductase R2 Proteins and Hemerythrin Produced by $\gamma$-Irradiation at 77 K

| protein | $g_\perp{}^a$ | $g_\parallel{}^b$ | $\Delta H_\parallel{}^c$ (mT) | reference |
|---|---|---|---|---|
| *E. coli* metR2 | 1.936 | 1.818 | 4.9 | Davydov et al. (1994) |
| mouse metR2 | 1.94 | 1.84, 1.79 | 4.6 | this work |
| HSV1 metR2 | 1.94 | 1.83 | 3.22 | this work |
| *E. coli* R2 Y122F | 1.937 | 1.809 | 5.2 | Davydov, R., et al. (1996) |
| *E. coli* R2 | 1.928 | 1.800 | 5.0 | Davydov, R., et al. (1996) |
| mouse R2 | 1.94 | 1.85, 1.82 | | this work |
| methemerythrin | 1.954 | 1.833 | | Davydov et al. (1994) |

[a] Measured at zero−crossing. [b] Measured at high-field minimum. [c] Half-width of high-field $g_\parallel$ feature.

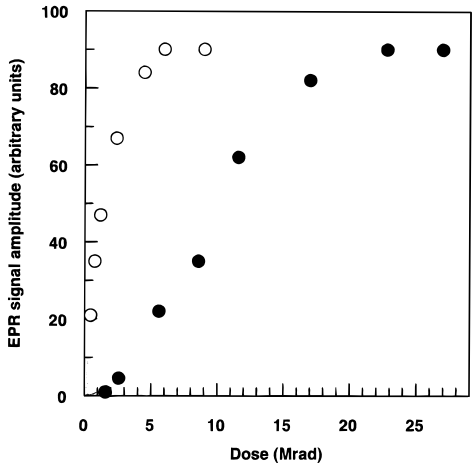


FIGURE 4: Relative EPR signal amplitude of the most high-field $g_\parallel$ feature for the primary mixed-valent species of mouse metR2 (○) and active mouse R2 (●) produced by irradiation at 77 K versus irradiation dose. Concentrations of mouse metR2 and active mouse R2 were 0.8 mM.

of the signal of Figure 3b indicates that about 15% of the diferric centers of HSV1 protein R2 have been reduced to a mixed-valent state by the $\gamma$-radiation at a dose of 4.6 Mrad at 77 K, and by subsequent annealing transformed into this final state. The EPR signal of Figure 3b, obtained after annealing at 250 K, is closely similar to that for the mixed-valent form of the protein generated at room temperature by photochemical (Figure 3c) or chemical reduction (Atta et al., 1994).

We have found no significant spectroscopic differences between the mixed-valent forms, produced at 77 K and by subsequent annealing at higher temperatures, in normal HSV1 protein R2 and in its truncated form lacking seven amino acid residues in the carboxyl terminus (data not shown).

*Effect of the Tyrosyl Radical on the Structure and Reactivity of the Diiron Center in Mouse R2 Protein.* The two components of the primary mixed-valent species in active mouse protein R2 trapped at 77 K display axial EPR signals with $g_\perp = 1.94$ (common for both) and $g_\parallel = 1.85$ and 1.82 for the two components, respectively (Figure 1b, Table 1). This spectrum is similar but not identical to that of the two primary mixed-valent components in mouse metR2. In the mixed-valent spectrum of active mouse R2 (Figure 1b), especially $g_\parallel$ features are markedly shifted to lower magnetic field (cf. Table 1).

Figure 4 shows the dependences of the intensity measured as signal amplitude of the primary mixed-valent signals (the

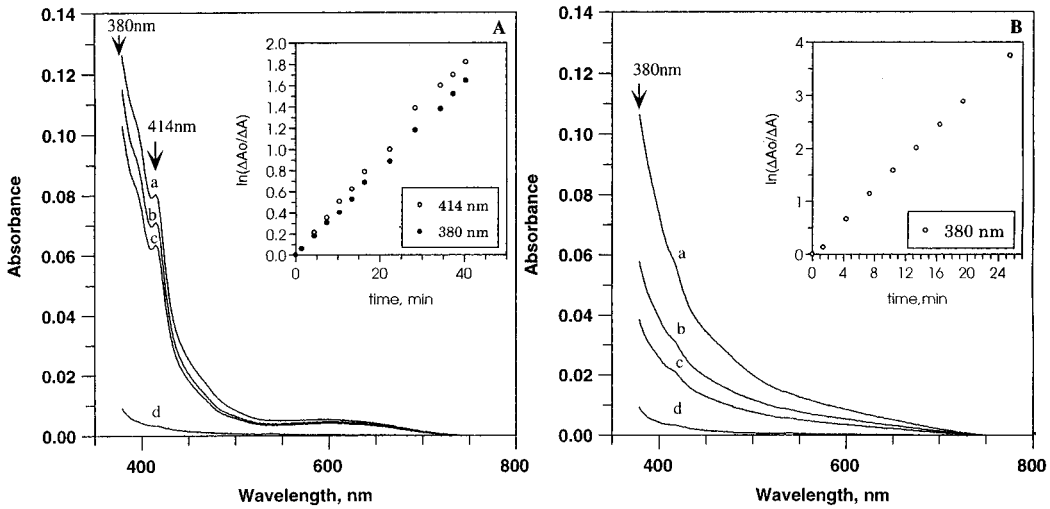


FIGURE 5: Reduction monitored by light absorption of active mouse R2 (panel A) and mouse metR2 obtained by treatment with 4-butoxyphenol (panel B) by 0.2 mM dithionite under anaerobic conditions. Experimental conditions: 11 $\mu$M active mouse R2 or mouse metR2 in 50 mM Tris-HCl, pH 7.6, 0.1 M KCl, 15 °C. Panel A: initial spectrum of active mouse R2 protein (a); after 2.5 min reaction with 0.2 mM dithionite (b); after 5 min (c); and after 40.4 min (d). Panel B: initial spectrum of mouse metR2 (a); after 4.4 min reaction with 0.2 mM dithionite (b); after 7.4 min (c); and after 25.4 min (d). Insets: logarithmic plots of the time dependence of the reduction reaction monitored at 380 nm and 414 nm (A) or 380 nm (B). $\Delta A_o$ is the difference between the absorbance before and after full reduction (traces a and d). $\Delta A$ is the difference between the absorbance at a given time and after full reduction.

most high-field $g_{||}$ features) as functions of radiation dose for the active and the met forms of mouse R2 protein. For each kind of protein, the two $g_{||}$ components show a similar dose dependence (data not shown). The results show that the yield of the mixed-valent species increases with irradiation dose in both active and met forms of mouse R2, but the shape of the yield vs dose curve is drastically affected by the presence of the tyrosyl radical. For the met form of mouse protein R2, the yield of the mixed-valent state increases steeply for small irradiation doses and reaches a plateau level already at 6 Mrad. When the tyrosyl radical is present at the beginning of irradiation, the active R2 case, the yield versus dose curve is sigmoidal with very small yields for low doses and leveling off first at doses above 20 Mrad (at high doses, the strong free radical signal in the irradiated sample of the active mouse R2 protein distorts the $g_{\perp}$ feature in the EPR spectrum of mixed-valent species Figure 1b). In the case of HSV1, there is a similar difference in dose curve shape between active and metR2 proteins, but the effect is much less marked (data not shown). These findings show that the presence of a tyrosyl radical influences the reactivity of the diferric center in a significant way.

We also followed the effect of the tyrosyl radical on the iron site reactivity by further studies on the chemical dithionite reduction of the diferric centers in the active and met forms of mouse R2 protein. Recently, we reported that, unlike in *E. coli* R2 protein, in mouse R2 both the diferric cluster and the tyrosyl radical are reduced by dithionite under anaerobic conditions (Davydov, A., et al., 1996). We have now studied the kinetics of these reduction reactions. Figure 5A,B shows the light absorption spectra of ~11 $\mu$M active and met mouse protein R2 during reduction by 0.2 mM dithionite. Under these conditions of excess dithionite, the reduction processes should follow pseudo-first-order kinetics. The insets in Figure 5 show that this is also the case. In the case of active protein, the absorbance losses at 414 nm, where the tyrosyl radical gives a major contribution, and at 380 nm, where the contribution of the diferric center dominates, follow pseudo-first-order kinetics (Figure 5A, inset) with similar rate constants estimated, 0.049 $min^{-1}$ and 0.042 $min^{-1}$, respectively. Under the same conditions, the pseudo-first-order rate constant for dithionite reduction of the diferric center in mouse metR2 is 0.157 $min^{-1}$, measured from the loss of absorbance at 380 nm (Figure 5B). These results suggest that the diferric site in mouse metR2 is more reactive toward dithionite than the site in active R2, as reflected by a ratio of about 4 between the rate constants. Similar differences in kinetics were observed also when using ascorbate as reductant. It should be noted that in the spectra of Figure 5B there is an extra absorbance centered at about 500 nm, which is not due to the diferric sites of mouse metR2, the spectrum of which should be completely below that of active R2. However, the contribution of this peak at 380 nm should be negligible. In addition, the rate of the absorbance decay at 500 nm is nearly the same as at 380 nm. Remaining 4-butoxyphenol and its oxidation product-(s) were not removed from the sample of mouse metR2, and the broad peak close to 500 nm should be due to these contaminants, since in a stock solution of 4-butoxyphenol we have observed a similar broad absorption.

Figure 6 shows a comparison of the light absorption spectra of mouse and *E. coli* metR2 proteins. The overall long-wavelength tails of the spectra are similar, but the spectrum of mouse metR2 is much less resolved. The derivatives shown in the inset, however, indicate the presence of optical bands at similar wavelengths in both proteins.

## DISCUSSION

*Presence of an Oxo Bridge in the Primary Mixed-Valent States.* The results demonstrate that $\gamma$-irradiation of mouse and HSV1 R2 proteins in a water−glycerol glass at 77 K gives rise to transient mixed-valent diiron intermediates in relatively high yields (15−20% of iron sites at a dose of 4.5 Mrad). The EPR spectra of the mouse and HSV1 protein R2 primary mixed-valent intermediates presented in Figure 1a,c, respectively, are similar to those of the corresponding species in *E. coli* protein R2 (Figure 1d) and methemerythrin (Davydov et al., 1994) (Table 1). This type of EPR signals with all *g*-values <2 in *E. coli* R2 was previously shown

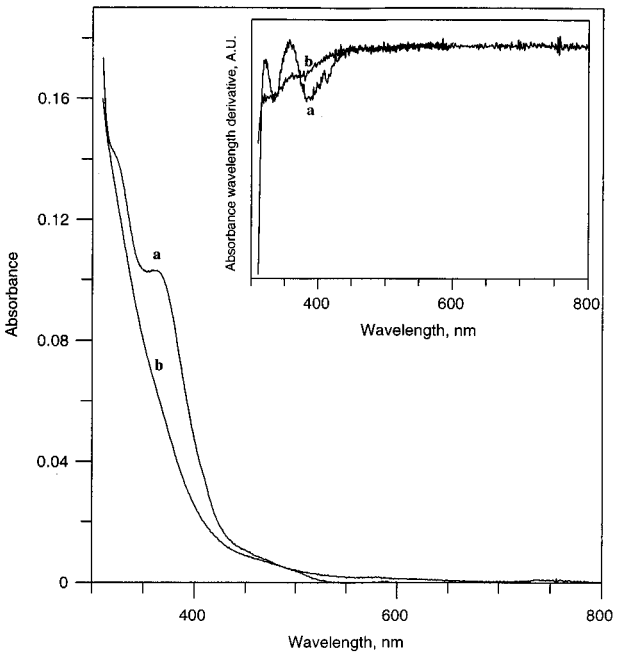


FIGURE 6: Light absorption spectra of 7 $\mu$M *E. coli* protein metR2 (a); and mouse metR2 (b). Inset: first derivatives of spectra a and b. The met form of mouse R2 protein was obtained by treatment of active mouse R2 with an equimolar (to the amount of tyrosyl radical) amount of 4-butoxyphenol at 4 °C.

(Davydov et al., 1994) to originate from $S = {}^1/_2$ antiferromagnetically coupled $\mu$-oxo-bridged Fe(II)/Fe(III) centers. Reduction at 77 K of these centers retains the coordination environment and geometry close to those of the initial diferric state. It has been previously shown that the EPR properties of the mixed-valent diiron clusters produced at 77 K in proteins and model compounds depend markedly on the nature of the bridging ligand (Davydov et al., 1994, 1995; Davydov, R., et al., 1996; Holz et al., 1993; Davydov, R., et al., 1997). Generally, the $\mu$-oxo-bridged mixed-valent clusters obtained by reduction at 77 K exhibit $S = {}^1/_2$ EPR spectra, with only a small spread in *g*-values (Davydov, R., et al., 1997). These spectra may be recorded at temperatures as high as 100−120 K (Davydov et al., 1994; 1995; Davydov, R., et al., 1997).

The primary mixed-valent species generated in methane monooxygenase by reduction of the $\mu$-hydroxo bridge with mobile electrons at 77 K gave a $\mu$-hydroxo-bridged mixed-valent diiron center (Davydov, A., et al., 1997). The same type of $\mu$-hydroxo-bridged mixed-valent diiron center has also been observed after chemical reduction in hemerythrin (DeRose et al., 1993; Vincent et al., 1990), MMO (DeRose et al., 1993; Vincent et al., 1990), and PAP (Thomann et al., 1993). These $\mu$-hydroxo-bridged mixed-valent species gave rise to $S = {}^1/_2$ EPR spectra with a large *g*-value anisotropy and were characterized by short spin relaxation times (the spectra could be observed only at $T < 25$ K). This clear difference beween $\mu$-oxo and $\mu$-hydroxo diiron clusters (Davydov, R., et al., 1997) is useful for interpretation of the present results in terms of the nature of the bridge in the diiron clusters of mouse and HSV1 proteins R2.

The effective *g*-values that characterize the primary mixed-valent species of RNR observed in this and earlier work (Davydov et al., 1994; Davydov, R., et al., 1996) are compiled in Table 1. The spin−lattice relaxation of all three species is comparatively slow: the spectra may be observed up to temperatures of 100 K. The $g_\perp$ and $g_{||}$ values fall in relatively narrow regions (cf. Table 1). We may conclude that the ligation and geometries of the diiron centers in the R2 proteins presented in Table 1 are quite similar but not identical and that they all have $\mu$-oxo bridges between the iron ions [cf. Davydov, R., et al. (1997)].

*Two Forms of Iron Sites in Mouse Protein R2.* There are distinct differences between EPR spectra of the primary mixed-valent species obtained from the three metR2 proteins (Table 1). Mouse metR2 reduced at 77 K gives a mixed-valent spectrum (Figure 1a) that may be interpreted as a superposition of signals from at least two mixed-valent components. Both show axial symmetry with identical or nearly identical $g_\perp$but different $g_{||}$ features. In active mouse R2, the mixed-valent EPR spectrum is also composed of two components, but neither of them coincides with the components observed for the met protein (Figure 1a,b; Table 1). This observation suggests that the $\mu$-oxo-bridged diferric sites in active mouse R2 are not identical to those in mouse metR2.

Active *E. coli* R2 is generally found to contain complete active sites, with tyrosyl radical, and met sites, without associated radical, in a ratio of 2:1 (Davydov, R., et al., 1996). In radiolytic reduction experiments at low temperature, it was found (Davydov, R., et al., 1996) that the met sites of active R2 were reduced as effectively as those of pure metR2, while an iron cluster of a complete site remained oxidized until its tyrosyl radical had been reduced. Correspondingly, the initial slopes of the yield versus dose curves of active R2 and metR2 were 1:3. From Figure 4, it is obvious that the amount of metR2 sites in the preparation of active mouse R2 is much smaller than in *E. coli* R2. The ratio of the initial slopes of the yield versus dose curves of active R2 and metR2 from mouse is between 1:50 and 1:100.

Taken together, these results suggest that in active mouse R2 the mixed valent EPR signals arise almost exclusively ($\geq$95%) from complete iron/radical clusters with a tyrosyl radical neighboring the iron site. These complete sites are clearly different, both spectroscopically and in terms of stability, from the diferric sites observed in mouse metR2. This conclusion is also supported by the higher rates of reduction observed for mouse R2 in the met form when compared to the active form (Figure 5).

The iron sites of mouse R2 give rise to two types of radiation-induced EPR spectra in the primary mixed-valent state in the met as well as in the active form of the protein. A similar heterogeneity in the primary mixed-valent EPR spectrum after low-temperature reduction was recently observed also in methane monooxygenase (Davydov, A., et al., 1997). In that case, the results were interpreted in terms of two distinct structures of the diferric site being present, as suggested by EXAFS studies (Shu et al., 1996). Also in the case of mouse R2 we may interpret our present observations in terms of two major structurally distinct forms of the iron site, probably due to somewhat different ligand arrangements. In HSV1 metR2, only one EPR spectral component is observed for the primary mixed-valent state (Figure 1c), similar to the situation in *E. coli* metR2.

Structural differences among the diferric sites in different R2 proteins are indicated by other spectroscopic studies (Mann et al., 1991; Thelander et al., 1994; Filatov et al., 1992; Sahlin et al., 1987; Lankinen et al., 1982; Ingemarson et al., 1989). The light absorption spectrum of the diferric

Table 2: Effective *g*-Values for the EPR Signals of the Mixed-Valent Intermediates Arising upon Annealing the Primary Mixed-Valent Forms of Mouse and HSV1 metR2 Proteins Produced at 77 K[a]

| protein R2 | $T_{an}$ | $g_1$ | $g_2$ | $g_3$ |
|---|---|---|---|---|
| mouse | 160 | 1.92 | 1.78 | 1.71 |
| HSV1 | 167 | 1.9 | 1.83 | 1.63 |
| mouse | 220 | 1.92 | 1.73 | 1.60 |
| HSV1 | 250 | 1.94 | 1.75 | 1.63 |

[a] The annealing was performed at the temperature $T_{an}$ for 3−10 min.

site in mouse metR2 is characterized by absorption bands at 320 and 370 nm (Figure 6) which are assigned to ligand-to-metal charge transfer from $O^{2-}$ to Fe(III). These bands are broadened and less intense as compared to those in the spectrum of *E. coli* metR2 (Figure 6). The antiferromagnetic coupling between the two iron(III) ions in *E. coli* R2 ($J = -98$ cm$^{-1}$) is markedly higher than in mouse ($J = -77$ cm$^{-1}$) and HSV1 R2 proteins ($J = -66$ cm$^{-1}$) (Galli et al., 1995). According to the calculations by McCormick et al. (1991), the observed differences between *g*-values for the primary mixed-valent signals may be interpreted by variations of both zero-field splitting and antiferromagnetic exchange coupling strength.

*Protonation of the Oxo Bridge after Annealing.* The results of annealing show that the primary mixed-valent forms of mouse and HSV R2 proteins are unstable and relax toward the respective equilibrium states. This transition proceeds via at least one EPR-distinguishable mixed-valent intermediate. In Table 2, the results of the present annealing experiments are compared with previous studies (Davydov et al., 1994; Davydov, R., et al., 1996). Annealing at 165 K of mouse and HSV1 primary mixed-valent species results in a stabilized secondary species with rhombic character and large *g*-value spread. At 220 K−250 K, the mixed-valent species of mouse and HSV1 proteins R2 relax further to their equilibrium states, which are closely similar to those obtainable by chemical reduction at room temperature. The EPR spectra of these final states have even larger *g*-value spreads and lower $g_{av}$ values (cf. Table 2). These equilibrium species have still more effective spin−lattice relaxation than the intermediate secondary species obtained after annealing at 165 K. The EPR spectra of the annealed samples cannot be observed above 25 K because of lifetime broadening. Taken together with previous results on mixed-valent forms obtained from methemerythrin (DeRose et al., 1993; Vincent et al., 1990; Davydov et al., 1994) and model diferric compounds (Davydov, R., et al., 1997), these observations indicate that the $\mu$-oxo bridge is protonated in the mixed-valent species obtained after annealing.

In Scheme 1, a plausible mechanism of relaxation for the primary mixed-valent forms is presented:

During annealing at 160−165 K of the primary mixed-valent species I, protonation of the $\mu$-oxo bridge and repositioning and reorientation of the ligands occur. The spectral differences between II and III observed after annealing above 220 K reflect further alterations in ligation geometry and/or ligand structure in the Fe(II)Fe(III) core until the final equilibrium state III is reached.

As shown previously (Davydov et al., 1994), the mixed-valent iron center in *E. coli* protein R2 behaves differently. Annealing at 165 K transforms the antiferromagnetically coupled species with $S = {}^1/_2$ into a ferromagnetically coupled species with $S = {}^9/_2$. Final annealing at 230 K makes the *E. coli* protein R2 sample EPR-silent.

Scheme 1

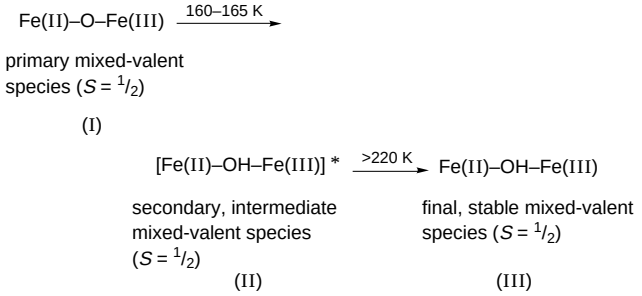


*Effect of the Tyrosyl Radical on the Structure and Reactivity of the Iron Site.* Previously we have shown that hydroxyurea-induced reduction of the tyrosyl radical in active *E. coli* R2 causes structural changes in the associated diferric center (Davydov, R., et al., 1996). The mutation Y122F in the protein has a strong effect on the redox potential (Silva et al., 1995) and the EPR properties of both the primary mixed-valent species produced at 77 K and the final mixed-valent state (Davydov, R., et al., 1996) (cf. Tables 1 and 2). The present observations show that reduction by chemical treatment of the tyrosyl radical in mouse protein R2 results in structural changes, which are revealed in the shapes of the mixed-valent EPR spectra obtained after low-temperature reduction (Figure 1, Table 1, cf. met and active R2). The structural changes in the diferric site induced by removing the tyrosyl radical in the protein are accompanied by a considerable increase in its rate of reduction by dithionite (Figure 5) and ascorbate.

We have found that the shape of the yield vs dose curve for the primary mixed-valent diiron centers depends on the presence of the radical (Figure 4). A similar effect of the tyrosyl radical on reduction of the diferric site at 77 K was reported for *E. coli* R2 protein (Davydov, R., et al., 1996). The results were interpreted in terms of electron transfer between the iron site and the radical. This route of electron transfer and the influence of the radical on the structure and reactivity of the diiron center may well have functional roles within the enzyme.

Previous studies on dinuclear iron sites in proteins have also suggested that the ligand arrangement may change depending on the redox state (Rosenzweig et al., 1993; Feig et al., 1994; Andersson et al., 1996). In the present case, the hydrogen-bonding network around the iron/radical site in R2 proteins may be different in the different red/ox states, and may be important for control of the reactivity of the site.

## REFERENCES

Andersson, K. K., & Gräslund, A. (1996) *Adv. Inorg. Chem. 43*, 359−405.

Atta, M., Lamarche, N., Battioni, J.-P., Massie, B., Langelier, Y., Mansuy, D., & Fontecave, M. (1993) *Biochem. J. 290*, 807−810.

Atta, M., Andersson, K. K., Ingemarson, R., Thelander, L., & Gräslund, A. (1994) *J. Am. Chem. Soc. 116*, 6429−6430.

Barlow, T., Eliasson, R., Platz, A., Reichard, P., & Sjöberg, B. M. (1983) *Proc. Natl. Acad. Sci. U.S.A. 80*, 1492−1495.

Davydov, A., Schmidt, P. P., & Gräslund, A. (1996) *Biochem. Biophys. Res. Commun. 219*, 213−218.

Davydov, A., Davydov, R., Gräslund, A., Lipscomb, J. D., & Andersson, K. K. (1997) *J. Biol. Chem. 272*, 7022−7026.

Davydov, R., Kuprin, S., Gräslund, A., & Ehrenberg, A. (1994) *J. Am. Chem. Soc. 116*, 11120−11128.
Davydov, R., Gräslund, A., Ehrenberg, A., Bowman, M., Smieja, J., & Dikanov, S. (1995) *J. Inorg. Biochem. 59*, 395.
Davydov, R., Sahlin, M., Kuprin, S., Gräslund, A., & Ehrenberg, A. (1996) *Biochemistry 35*, 5571−5576.
Davydov, R., Menage, S., Fontecave, M., Gräslund, A., & Ehrenberg, A. (1997) *J. Biol. Inorg. Chem. 2*, 242−255.
DeRose, V. J., Liu, K. E., Kurtz, D. M., Jr., Hoffman, B. M., & Lippard, S. J. (1993) *J. Am. Chem. Soc. 115*, 6440−6441.
Ericsson, S., & Sjöberg, B.-M. (1989) in *Allosteric Enzymes* (Herve, G., Ed.) pp 189−215, CRC Press, Boca Raton, FL.
Feig, A. L., & Lippard, S. (1994) *J. Chem. Rev. 94*, 759−805.
Filatov, D., Ingemarson, R., Gräslund, A., & Thelander, L. (1992) *J. Biol. Chem. 267*, 15816−15822.
Fontecave, M., Nordlund, P., Eklund, H., & Reichard, P. (1992) *Adv. Enzymol. Relat. Areas Mol. Biol. 65*, 147−183.
Galli, C., Atta, M., Andersson, K. K., Gräslund, A., & Brudvig, G. W. (1995) *J. Am. Chem. Soc. 117*, 740−746.
Hales, B. J. (1993) *Methods Enzymol. 227*, 384−395.
Holz, R. C., Elgren, T. E., Pearce, L. L., Zhang, J. H., O'Connor, C. J., & Que, L., Jr. (1993) *Inorg. Chem. 115*, 5844−5850.
Ingemarson, R., Gräslund, A., Darling, A., & Thelander, L. (1989) *J. Virol. 63*, 3769−3776.
Kauppi, B., Nielsen, B. B., Ramaswamy, S., Kjøller Larsen, I., Thelander, M., Thelander, L., & Eklund, H. (1996) *J. Mol. Biol. 262*, 706−720.
Lankinen, H., Gräslund, A., & Thelander, L. (1982) *J. Virol. 41*, 893−900.
Lassmann, G., Thelander, L., & Gräslund, A. (1992) *Biochem. Biophys. Res. Commun. 188*, 879−887.
Mann, G. F., Gräslund, A., Ochiai, E.-I., Ingemarson, R., & Thelander, L. (1991) *Biochemistry 30*, 1939−1947.
McClarty, G. A., Chan, A. K., Choy, B. K., & Wright, J. A. (1980) *J. Biol. Chem. 265*, 7539−7547.
McCormick, J. M., Reem, R. C., & Solomon, E. I. (1991) *J. Am. Chem. Soc. 113*, 9066−9079.
Nordlund, P., & Eklund, H., (1993) *J. Mol. Biol. 232*, 123−164.
Nordlund, P., Sjöberg, B.-M., & Eklund, H. (1990) *Nature 345*, 593−598.
Nyholm, S., Thelander, L., & Gräslund, A. (1993) *Biochemistry 32*, 11569−11574.
Reichard, P. (1988) *Annu. Rev. Biochem. 57*, 349−374.
Reichard, P. (1993) *Science 260*, 1773−1776.
Rosenzweig, A. C., Frederick, C. A., Lippard, S. J., & Nordlund, P. (1993) *Nature 366*, 537−543.
Sahlin, M., Gräslund, A., & Ehrenberg, A. (1986) *J. Magn. Reson. 67*, 135−137.
Sahlin, M., Peterson, L., Gräslund, A., Ehrenberg, A., Sjöberg, B.-M., & Thelander, L. (1987) *Biochemistry 26*, 5541−5548.
Shu, L., Liu, Y., Lipscomb, J. D., & Que, L., Jr. (1996) *J. Biol. Inorg. Chem. 1*, 297−304.
Silva, K. E., Elgren, T. E., Que, L., & Stankovich, M. T. (1995) *Biochemistry 34*, 14093−14103.
Stubbe, J. (1990) *Adv. Enzymol. Relat. Areas Mol. Biol. 63*, 349−419.
Thelander, L., & Gräslund, A. (1994) *Met. Ions Biol. Syst. 30*, 109−129.
Thomann, H., Bernardo, M. M., McCormick, J. M., Pulver, S., Andersson, K. K., Lipscomb, J. D., & Solomon, E. I. (1993) *J. Am. Chem. Soc. 115*, 8881−8882.
Vincent, J. B., Olivier-Lilley, G. L., & Averill, B. A. (1990) *Chem. Rev. 90*, 1447−1467.

BI9700375